SPACE RESEARCH COORDINATION CENTER

KINETICS AND MECHANISM OF NO_2 FLUORESCENCE

BY

L. F. KEYSER, S. Z. LEVINE AND
F. KAUFMAN

DEPARTMENT OF CHEMISTRY

SRCC REPORT NO. 134

UNIVERSITY OF PITTSBURGH

PITTSBURGH, PENNSYLVANIA

4 AUGUST 1970

The Space Research Coordination Center, established in May, 1963, has the following functions: (1) it administers predoctoral and postdoctoral fellowships in space-related science and engineering programs; (2) it makes available, on application and after review, allocations to assist new faculty members in the Division of the Natural Sciences and the School of Engineering to initiate research programs or to permit established faculty members to do preliminary; work on research ideas of a novel character; (3) in the Division of the Natural Sciences it makes an annual allocation of funds to the interdisciplinary Laboratory for Atmospheric and Space Sciences; (4) in the School of Engineering it makes a similar allocation of funds to the Department of Metallurgical and Materials Engineering and to the program in Engineering Systems Management of the Department of Industrial Engineering; and (5) in concert with the University's Knowledge Availability Systems Center, it seeks to assist in the orderly transfer of new space-generated knowledge in industrial application. The Center also issues periodic reports of space-oriented research and a comprehensive annual report.

The Center is supported by an Institutional Grant (NsG-416) from the National Aeronautics and Space Administration, strongly supplemented by grants from the A. W. Mellon Educational and Charitable Trust, the Maurice Falk Medical Fund, the Richard King Mellon Foundation and the Sarah Mellon Scaife Foundation. Much of the work described in SRCC reports is financed by other grants, made to individual faculty members.

KINETICS AND MECHANISM OF NO_2 FLUORESCENCE*

L. F. Keyser,† S. Z. Levine, and F. Kaufman

Department of Chemistry
University of Pittsburgh
Pittsburgh, Pa. 15213

Abstract

NO_2 fluorescence experiments with steady or modulated (8 and 20 kHz), monochromatic excitation at 4000 to 6000Å and monochromatic observation have shown the process to be interpretable in terms of a single electronically excited state undergoing vibrational relaxation at gas-kinetic rate and electronic quenching about 100 times more slowly. An apparent radiative lifetime of about 55 μsec was found, independent of excitation frequency, but the possibility of mixing with vibrationally excited ground state makes this an upper limit to the lifetime of the hypothetical unperturbed $^2B_1$ state. The average amount of vibrational energy transferred per collision was found to be 1000 ± 500 cm^{-1} based on a simplified stepladder model for the relaxation.

Introduction

Investigation of the visible absorption and fluorescence of NO_2 has presented several interesting theoretical and experimental problems in recent years. As is well known, the visible spectrum of NO_2 is extensive

and very complicated, and only recently have parts of it been successfully analyzed. Measurements of the fluorescence decay rate have resulted in a value of the radiative lifetime more than two orders of magnitude in excess of the lifetime calculated from the integrated absorption coefficient. The complicated spectrum and the anomolously long lifetime have led to much discussion of the number of states involved in the visible transition and the possible mechanisms which could account for such a large lifetime difference. In addition, studies of the fluorescence quenching have suggested that measurable vibrational relaxation occurs in excited NO_2. Measurements of NO_2 fluorescence are also of interest because of their relation to the chemiluminescent reactions of NO with O or O_3 in which excited NO_2 is the emitting species.

The ground state of NO_2 has been well characterized by infrared and microwave spectroscopy and is reasonably well understood theoretically as well. However, the visible absorption spectrum has been a formidable problem for many years and only recently have advances been made in its interpretation[1]. Calculations of the low lying electronic states have been carried out using nonempirical methods by Burnelle et al.[2] and by Fink[3]. The results indicate that five states, $^2B_1$, $^2B_2$, $^2A_2$, $^4A_2$, $^4B_2$, lie in the energy range 2 to 4 eV above the ground $^2A_1$ state and could be involved in the visible system; however, allowed transitions occur from $^2A_1$ only to $^2B_1$ and $^2B_2$. The calculated vertical transition energy for $^2B_2$ is 4.1 eV, but the calculations do not appear to be sufficiently accurate at present to decide whether this state is responsible for the ultraviolet absorption between 4.8 and 5.3 eV or also contributes to the visible spectrum. For $^2B_1$ the calculated vertical transition energy is 2.1 to 2.3 eV and the state

must contribute to the visible spectrum. Douglas and Huber's[1] rotational analysis of bands appearing in the absorption spectrum near 3 eV have identified the transition as $^2B_1 \leftarrow {}^2A_1$. Thus, from present evidence, it appears that the main intensity of the visible spectrum can be assigned to the transition to the $^2B_1$ state, which, to account for the complicated nature of the spectrum, is most likely perturbed by interaction with the other low lying states or by interaction with the ground state itself.

In a study of NO_2 fluorescence using flash excitation, Neuberger and Duncan[4] observed a 44 μsec radiative lifetime independent of the excitation wavelength between 3950 and 4650Å. The lifetime calculated from the absorption coefficient measurements of Hall and Blacet[5] and of Dixon[6] is about 0.3 μsec, more than two orders of magnitude shorter than the observed emission lifetime. This large lifetime anomaly has led to speculation[4,7] that more than one electronic state may be involved in NO_2 chemiluminescence and fluorescence. However, it has been pointed out by Douglas that this type of anomaly may be due to several causes, among them the interaction between vibrational levels of the excited electronic state with other states, and Hartley and Thrush[9] have suggested that highly excited vibrational levels of the ground electronic state may be partly responsible.

In previous experiments on NO_2 fluorescence, Myers, Silver, and Kaufman[10] reported a large decrease in the Stern-Volmer quenching constant with increasing energy separation between exciting and fluorescent radiation; this suggested that stepwise vibrational deactivation occurs in the excited electronic state. More recently, Sakurai and Broida[11] have studied NO_2 fluorescence using laser excitation; they observed a series of lines superimposed on what appeared to be a continuum with the resolution used. Quenching constants

obtained for the lines and the integrated continuum are somewhat uncertain but lie in the same range of values reported previously for NO_2 fluorescence [10,12]. Relative intensity variations with NO_2 pressure were interpreted in terms of collisional deactivation in the upper state.

The purpose of the present investigation was to study the vibrational deactivation of excited NO_2 in more detail and to determine the possible contribution of more than one electronic state to NO_2 fluorescence. A preliminary report of our results has been published[13]. While this work was in progress, we learned of parallel experiments on NO_2 fluorescence by Schwartz and Johnston[14], who used a similar experimental approach. However, the results of our measurements differ somewhat from theirs and it was thought appropriate to report them here in some detail.

In the following sections we first report the results of fluorescence experiments with steady illumination at a series of excitation and fluorescent wavelengths in the visible and near infrared regions and discuss the results in terms of a vibrational cascade model. Then, results are given of radiative lifetime measurements using modulated radiation at several excitation wavelengths and modulation frequencies.

Experimental

The system used in these experiments is shown schematically in Figure 1. Fluorescence is excited by means of a 500 watt high pressure mercury arc (Osram HBO-500) or 900 watt xenon arc (Osram XBO-900) powered by a standard d.c. power supply with added filtering to reduce the 60 Hertz ripple below 2%. After collimation, the exciting light is modulated using a

mechanical chopper which consists of two quartz disks (Dynamics Research Corp., Stoneham, Mass.) on each of which 512 slits had been formed by metallic deposition. One of the disks is stationary; the other is rotated at a constant speed by a d.c. motor powered by a regulated voltage supply, and the two disks are mounted 0.15 mm apart. The motor speed is continuously variable up to a maximum of 5000 rpm; this provides modulation frequencies from 2 kHertz up to 40 kHertz. Most of the present experiments on NO_2 were done at 8 or 20 kHertz. For experiments with steady illumination, the modulator is removed from the light path. The wavelength of the exciting radiation is varied by means of a 1/4 meter Jarrell-Ash monochromator; 500 μ slit widths are used, giving full band widths at half height of about 30Å. After emerging from the monochromator, the exciting light beam is collimated so that it is approximately 1 cm in diameter as it passes through the fluorescence cell. A 1P28 photomultiplier tube is used to monitor the intensity of the exciting light; it also provides the reference signal for the lifetime measurements.

Fluorescence signals are observed at right angles to the exciting beam through the side window of a glass T-shaped cell 24 cm in length with an inside diameter of 14 cm. The wavelength at which fluorescence is observed is varied by using a set of interference filters (Thin Film Products, Inc.) or Corning glass filters placed between the cell and the PMT detector. The transmission wavelengths of the interference filters are spaced at 300-600Å intervals in the visible and near infrared; the filters have a 50-75Å band width at half maximum transmission.

An EMR 641E photomultiplier tube is used to detect the fluorescence signal. This tube has an S-20 response with a quantum efficiency of 11% at

6300Å; for most experiments, it is operated at a gain of 10^7 which gives a dark current of 3×10^{-12} amps or 2-3 photon pulses per second when cooled. The 641E tube is housed in an evacuable metal dewar and cooled radiatively by a copper heat shield at -77°C.

In the experiments using unmodulated exciting light, the 641E output is amplified (Keithley 417 picoammeter) and displayed on a strip chart recorder (Bausch & Lomb VOM5). At very low fluorescence intensities (low pressure and long excitation wavelength), the fluorescence signal is measured in digital form by means of a pulse amplifier at the 641E output, pulse height discriminator, and electronic counter. Counting times of 10 sec are adequate to obtain significant fluorescent intensity signals.

For the lifetime measurements the pulse counting detection system is used; a schematic diagram of the experimental arrangement is shown in Fig. 2. The output of the 1P28 triggers a variable delay pulse which starts a time to amplitude converter (E.G.&G. TH200A modified to give a 130 μsec ramp for 8 kHertz modulation). A start pulse is generated once during each modulation cycle and at a known phase with respect to the exciting light as observed on a dual trace oscilloscope. After amplification and low level discrimination, the output pulses of the 641E are fed to the time to amplitude converter. The first photon pulse subsequent to the start pulse stops the ramp and the resulting voltage pulse is transmitted to a multichannel analyzer where the fluorescent wave form is stored for later processing. For most experiments counting times of 10 minutes (real time) are sufficient to accumulate fluorescence signals with an average of 500 counts per 1.5 μsec time channel. The time base of the analyzer is calibrated vs. a time mark generator. Using this method of detection, no

more than one fluorescence photon pulse may be counted during each cycle of the exciting light modulation; thus, distortion of the detected signal wave form will occur if the average counting rate approaches the modulation frequency. The highest counting rate used in these experiments is 600 counts per sec which is sufficiently low compared to the lowest modulation frequency (8 kHertz) that distortion effects may be ignored. The phase shift introduced by the detection system itself is established by measuring the phase of scattered light with no NO_2 in the cell. An electronic counter (Hewlett-Packard 5512A) is used to measure photon counting rates and the modulation frequency.

Pressures of NO_2 in the range 0.5 to 500 mTorr are measured with a pressure transducer (Pace P90D) which is calibrated against a McLeod gauge using helium gas to minimize the mercury streaming effect[15]. The NO_2 obtained from Matheson at a stated purity of 99.5% is further purified by reaction with excess oxygen gas followed by several sublimations at -77°C. The purified NO_2 is stored in the dark at -196°C. At the start of each set of experiments, a fresh sample of NO_2 is distilled from the storage bulb into a separate trap at -77°C from which it is admitted to the fluorescence cell as needed. During an experimental run, the cell and one side of the pressure transducer are isolated from the remainder of the NO_2 handling system by means of a stainless steel bellows valve. Typical pressure increases in the isolated cell are less than 0.1 mTorr per hour.

Steady Excitation

Fluorescence of NO_2 was excited by steady illumination at a series of wavelengths, λ_E = 4050, 4360, 5460, and 5780Å; for each exciting wavelength,

the fluorescent intensity was determined as a function of NO_2 pressure and fluorescent wavelength out to 7850Å. The data of each experiment consist of 40 to 50 intensity vs. pressure readings over a pressure range of 0.5 to 125 mTorr. Representative Stern-Volmer plots of the results for 4358Å excitation are shown in Fig. 3, where for clarity only three fluorescent wavelengths have been included. Results at other fluorescent wavelengths lie between the curves shown. Similar curves are obtained at other excitation energies.

The Stern-Volmer[16] model of fluorescence quenching considers only one excited level which after formation by photon absorption may radiate or be collisionally quenched to the ground level. Under steady-state conditions, the following relation is easily obtained

$$P/F = B(1 + aP) \tag{1}$$

where P is the NO_2 pressure; F, the fluorescent intensity; a, the quenching constant, defined as the ratio of the quenching rate constant, E, to the radiative rate constant, R; and B is an experimental constant which includes such factors as the absorption cross section, the exciting light intensity, and the efficiency of the optical system used to detect the fluorescence. To facilitate comparison of experimental results at different exciting and fluorescent wavelengths, B is determined for each combination of λ_E and λ_F by linear extrapolation of P/F vs. P plots to zero pressure.

Examination of the quenching results shown in Fig. 3, where P/BF is plotted vs. P, shows that the experimental plots are linear throughout the pressure range only if the fluorescence frequency, ν_F, is close to the exci-

tation frequency ν_E. At low NO_2 pressures, the results show increasing curvature as $\Delta\nu = \nu_E - \nu_F$ increases. At higher NO_2 pressures (above 10 to 20 mTorr) the curves become linear and it is possible to obtain an effective quenching constant from the high pressure slope. Observed quenching constants for various exciting and fluorescent wavelengths are given in Table I. As $\Delta\nu$ increases, a sharp decrease in the magnitude of the quenching constant is observed, the variation being as large as a factor of five over the range of $\Delta\nu$ observed. Within experimental scatter, the quenching constants are dependent only on $\Delta\nu$ and appear to be independent of the value of ν_E or ν_F.

The results summarized above show that a simple Stern-Volmer description with only one excited level is not applicable to the visible fluorescence of NO_2 because (1) the quenching curves (Fig. 3) deviate substantially from linearity for NO_2 pressures below 20 mTorr[17] and (2) the observed quenching constants show a strong dependence on $\Delta\nu$. These observations suggest a cascade model with stepwise vibrational de-excitation in a single excited electronic state of NO_2 concurrent with its electronic and radiative de-excitation. Such a vibrational cascade model may be described in terms of the following equations,

$$\frac{-d\,M_1}{dt} = (R + EM + VM)\,M_1 - A\,I_e M$$

$$\frac{-d\,M_2}{dt} = (R + EM + VM)\,M_2 - VMM_1$$

$$\frac{-d\,M_i}{dt} = (R + EM + VM)\,M_i - VM\,M_{i-1} \qquad (2)$$

where M is the ground state population density of the fluorescent molecule,

the M_i's are the population densities of excited levels, R is the radiative rate constant, E is the electronic quenching rate constant, V is the vibrational quenching rate constant, A is the absorption coefficient, and I_e is the intensity of the exciting light. In Eqs. (2), a number of simplifying assumptions have been made:

(1) The rate constants are independent of the particular level of excitation, i.e. $R_1 = R_2 = R_i = R$, $E_1 = E_2 = E_i = E$, and $V_1 = V_2 = V_i = V$. This is suggested by the relative independence of the observed quenching constants on the value of ν_E for a given $\Delta\nu$. For R_i, moreover, this constancy is further supported by the lifetime measurements discussed below.

(2) The only energy transfer or loss processes important in the present case are those described by Eqs. (2). This ignores diffusive loss, radiative transfer among the excited vibrational levels, and collisionally induced vibrational excitation, all of which should be relatively unimportant compared to the rates R, E, and V.

(3) All the excited state levels lying within $\Delta\nu$ of ν_E contribute to the fluorescent intensity in proportion only to their relative population densities. This ignores the fluorescent spectral distribution which was shown to have relatively little effect on the calculated results of the simplified model by specifically including in one of the calculations a scaled spectral distribution similar to that of the O + NO emission[18].

Under steady-state conditions, the population densities in the excited levels may be readily obtained:

$$M_1 = (A\, I_e/R)\, \left[\frac{M}{1 + (a_E + a_V)M}\right]$$

$$M_i = \left[\frac{a_V M}{1 + (a_E + a_V)M}\right] M_{i-1} \qquad (3)$$

where $a_E = E/R$ and $a_V = V/R$ are the electronic and vibrational quenching constants. Using the above assumptions, the fluorescent intensity may be summed over all excited levels and the result is given by:

$$P/F = B\, (1 + a_V SP)/\{1 - \left[\frac{a_V P}{1 + a_V(1+S)P}\right]^n\} \qquad (4)$$

where F is the total fluorescent intensity, B is an experimental constant previously defined, $S = a_E/a_V = E/V$, and the ground state population density has been replaced by the corresponding pressure, P. The exponent n represents the number of excited levels which contribute to the fluorescent signal; this number depends on the average size of the vibrational quantum transferred per quenching collision, $\Delta\nu_{vib}$, and on the energy separation between the exciting and fluorescent light; i.e., n may be written as

$$n = 1 + (\nu_E - \nu_F)/\Delta\nu_{vib}. \qquad (5)$$

At sufficiently high pressures, $P >> 1/a_V$; Eq. (4) becomes linear in P,

$$P/F = B\, a_V\, P\, S\, (1 + S)^n/[(1 + S)^n - 1] \qquad (6)$$

and the observed quenching constants defined above and given in Table I can then be written as

$$a_{obs} = a_V S (1 + S)^n/[(1 + S)^n - 1] = a_V G(n,S) \qquad (7)$$

The factor G(n,S) has been evaluated for various values of n and S and the results are given in Table II, where an increase in n for fixed S corresponds to experimentally increasing $\Delta\nu$. Examination of Table II shows that in order to account for the large variation in a_{obs}, S must be 0.10 or less; that is, the vibrational quenching rate must be considerably faster than electronic quenching in excited NO_2.

A more detailed comparison of the calculated and experimental quenching constants is shown in Fig. 4, where relative values of the quenching constants are plotted vs. $\Delta\nu$. To obtain the calculated curves, values of $\Delta\nu_{vib}$ are chosen between 500 and 2000 cm^{-1}; and S is varied between 0.1 and and 0 ($a_E = 0$). For a given $\Delta\nu_{vib}$, n is calculated using Eq. (5), and the relative quenching constants can then be obtained from Table II. While the best overall agreement occurs at $\Delta\nu_{vib} = 1000 \pm 500$ cm^{-1}, the experimental scatter and relative insensitivity of the calculation to variation in S at low values, permit only a choice of an upper bound for S, that is, $S \leq 0.01$. For $\Delta\nu_{vib} = 1000$ cm^{-1} and $S = 0.01$, a_V can be obtained from the observed quenching constants using Eq. (7) and the values of G(n,S) in Table II. The average value of a_V obtained in this way is about 700 $Torr^{-1}$; a_E is then 7 $Torr^{-1}$. Quenching rate constants may then be obtained from the definition of a_V if the radiative lifetime is known. Taking $\tau_R = 5.5 \times 10^{-5}$ sec (see following Section), $E = 3.9 \times 10^{-12}$ and $V = 3.9 \times 10^{-10}$ cm^3/molecule-sec. At low values of S, V is approximately independent of S while E varies as S; thus for values of S less than 0.01, V differs little from the value given above.

Quenching curves calculated from Eq. (4) for $\Delta\nu_{vib} = 1000\ cm^{-1}$ and S = 0.01 are compared with experimental points in Fig. 3; the agreement is very good considering the many approximations of the model. However, the calculated curves are also insensitive to the choice of S at low values and cannot be used to determine this parameter beyond the previously established limit of $S \lesssim 0.01$.

Fluorescence Lifetime

The lifetime of NO_2 fluorescence excited at several wavelengths was determined by means of the phase-shift method[19]. For the lifetime experiments, modulated exciting light is used; the intensity is given by

$$I_e(t) = \tilde{I}_e [1 + m \cos (\omega t - \phi_0)] \qquad (8)$$

where ω is the angular frequency of modulation, $\tilde{I}_e$ is the average exciting light intensity (d.c. level), m is the fraction of modulation defined as the ratio of maximum amplitude to the d.c. level, and ϕ_0 is the zero or reference phase of the system. Only the fundamental Fourier component is included in the discussion; Fourier analysis of the experimental results shows that the fundamental accounts for approximately 90% of the amplitude in both the excitation and fluorescent waveforms.

When the frequency separation between the exciting and the fluorescent radiation, $\Delta\nu$, is small, or for any $\Delta\nu$ at sufficiently low pressures, only one upper level contributes to the observed fluorescent signal. At low pressure, the time variation in the fluorescent signal may be obtained by

solving Eqs. (2) for i = 1 with I_e given by Eq. (8). The fluorescent signal may then be written

$$F(t) = \tilde{F} [1 + \lambda m \cos (\omega t - \Delta\phi)] \tag{9}$$

where the phase angle, $\Delta\phi$, by which the phase of the observed fluorescent signal is shifted with respect to ϕ_0, is simply related to the lifetime, τ, by

$$\tan \Delta\phi = \omega\tau \tag{10}$$

and

$$\tau^{-1} = \tau_R^{-1} [1 + (a_E + a_V) P]. \tag{11}$$

The fraction of modulation in the fluorescent signal is attenuated by the factor λ, where

$$\lambda = (1 + \omega^2 \tau^2)^{-1/2}. \tag{12}$$

Eqs. (10) and (12) show that either the phase shift or the attenuation factor can be used to measure the lifetime; however, the phase shift is the more accurately measured and this is the method used here.

A representative fluorescent waveform is shown in Fig. 5, where the counts per channel are plotted vs. time since the start trigger. To obtain the phase shift, the reference phase of the system is established by record-

ing the exciting light waveform with no NO_2 in the cell. Both the fluorescent and the exciting light signals are corrected for a small dark current background and the fluorescent signal is corrected for scattered light[19]. Both waveforms are expanded in a Fourier series (up to the fifth harmonic) and the resulting fundamental coefficients are used to determine the phase shift by computer analysis.

Typical results of lifetime measurements using 8 kHertz modulation at low NO_2 pressures are shown in Fig. 6. Table III summarizes the results; the radiative lifetimes and quenching constants were obtained from a linear least squares fit of the experimental data. In experiments where $\Delta\nu$ is large or where sharp cut filters were used in the fluorescent beam, the $1/\tau$ vs. P plots were non-linear and τ_R was obtained from an extrapolation of the low pressure points. Errors quoted are the standard deviations obtained from the least squares analysis. Quenching constants obtained from the steady illumination experiments (Table I) are in satisfactory agreement with these results where conditions are comparable.

Frequency Variation

Variation of the modulation frequency may be used to determine whether a portion of the NO_2 visible fluorescence is due to emission from a state with a much shorter lifetime than 55 μsec. If only one state contributes to the fluorescence, the observed lifetime is independent of the modulation frequency ω; however, if there are two or more excited states involved, the observed lifetime varies with ω. At low ω, the observed phase shift is due mainly to relatively long-lived states; but as ω increases, the long-lived states cannot follow the rapid modulation and the observed phase shift is

due mainly to the short-lived states. Thus, the observed lifetime should decrease with increasing ω if a short-lived state contributes to the NO_2 fluorescence.

If emission occurs concurrently from two excited states, the following relation between the observed lifetime, τ_{obs}, and the lifetimes of the excited states, τ_1 and τ_2, is obtained:

$$\tau_{obs} = \frac{(1 + \omega^2\tau_2^2)\, P_1\, \tau_1 + (1 + \omega^2\tau_1^2)\,(1 - P_1)\,\tau_2}{(1 + \omega^2\tau_1^2)(1 - P_1) + (1 + \omega^2\tau_2^2)\, P_1} \qquad (13)$$

where P_1 and $(1 - P_1)$ represent the fraction of fluorescent intensity due to state 1 and state 2 respectively. Using the measured value of 55 μsec for τ_1, and for τ_2 a value of 0.25 μsec calculated[4] from the absorption coefficient, τ_{obs} as a function of ω is shown in Fig. 7 for various values of P_1. At higher modulation frequencies the phase-shift measurement becomes sensitive to the presence of even small contributions from a relatively short-lived state; for example, with a change in frequency from 8 to 20 kHertz, the observed lifetime should change by a factor of about 1.4 if 1% of the fluorescent intensity comes from a state with 0.25 μsec lifetime.

As shown in Table III, there is no significant change in lifetime as the frequency is varied; the average observed lifetime at 8 kHertz is 56 μsec, while at 20 kHertz it is 54 μsec. This shows that the visible NO_2 fluorescence originates from one excited state with a lifetime of 55 μsec; and as seen in Fig. 7, any contribution from a separate short-lived state must be considerably less than 1% of the total intensity.

Discussion

The combined results of the steady and the modulated excitation experiments indicate that NO_2 fluorescence involves a single electronically excited state in which efficient vibrational relaxation occurs at approximately gas kinetic rate, $V = 3.9 \times 10^{-10}$, compared to about 2×10^{-10} cm^3/molecule-sec for the gas kinetic collision rate of ground-state NO_2. However, electronic quenching requires about a hundred collisions. The size of the vibrational quantum transferred per quenching collision, 1000 ± 500 cm^{-1}, is in the range of the 880 cm^{-1} bending frequency of excited NO_2 [1]. Observation of rapid collisional quenching in excited NO_2 is consistent with the results of studies in SO_2 fluorescence where rapid vibrational relaxation has also been reported[20,21].

No significant variation in the fluorescent lifetime was observed for excitation energies from 16,700 to 24,700 cm^{-1}, which further argues against the existence of a short-lived state. If more than one state were involved, the relative contributions of the excited states may be expected to change with excitation energy and lead to a large variation in the observed lifetime. The conclusion of only one emitting state is thus supported by the frequency variation experiments, by the excitation energy experiments, and by the very direct result of Douglas[8] that, after sudden cut-off from steady illumination, the total fluorescence intensity decayed with a single lifetime of about 50 μsec.

Other investigators[4,8,14] have also reported lifetimes from 44 to 90 μsec. Our work is, however, in disagreement with the sharply fluctuating τ_R (between 60 and 90 μsec) as function of ν_E of Schwartz and Johnston[14] (SJ). As these results of SJ were obtained with a Corning 2-73 or other

sharp-cut filters in the fluorescent beam whereas ours were usually obtained with an interference filter of wavelength close to that of the exciting light, we carried out a few experiments under conditions closely matching those of SJ and corresponding to their sharp peaks of τ_R at 5600 and 6000Å excitation. The results in Table III show no appreciable change of τ_R. It should also be emphasized (a) that SJ's lifetimes (Fig. 3) were obtained at an NO_2 pressure of 1.3 mTorr whereas ours are radiative lifetimes at zero pressure extrapolated from 20 to 30 experiments at pressures of 1 to 15 mTorr. This widens the discrepancy by about 50%, since SJ's lifetimes are to be increased by about 30% using the slopes of our $1/\tau$ vs. P curves; (b) our lifetimes are based on a full waveform analysis of each experiment whereas SJ's are based only on the intensities of in phase and out of phase components of the fluorescence. Still, the origin of the discrepancy is unclear, but the present results, viz. the insensitivity of τ_R to small variations of ν_E, seem reasonable.

The magnitude of τ_R is also affected by the size of the fluorescence cell and of the optical region of observation, because the excited molecules move an appreciable distance before radiating. The effective observation diameter used by SJ was 20 cm in a cell of 33 cm diameter whereas our observation was confined to 8 cm in a cylindrical 14 cm cell. Both SJ's (Table I) and our results with various cell sizes would suggest that this effect may increase our τ_R by only $\lesssim$ 10%.

There is good agreement with SJ's estimate of the vibrational relaxation rate constant (4×10^{-10} cm^3/sec) and satisfactory agreement with their electronic quenching ($\lesssim 2 \times 10^{-11}$ cm^3/sec) and energy removed per collision (2000 - 4000 cm^{-1}). The latter seems too large in view of findings of chem-

ical activation experiments for larger molecules[22].

Interaction of excited electronic levels of NO_2 with upper vibrational levels of the ground electronic state (or of other non-radiating electronic states) is a possible explanation of the long radiative lifetime of NO_2. This type of interaction has been suggested by several authors[8,9] and possible mechanisms have been discussed[23,24]. Interaction leads to the establishment of an equilibrium between the levels (assuming that the crossing rate is greater than the deactivation rate or that the electronic states are truly mixed), and since at equal energies the density of levels is much greater in the ground than in the excited electronic state, the equilibrium assumption decreases the true radiative lifetime of the excited state by the factor K + 1, where K is the ratio of level densities of ground and excited states, because the observed radiative decay includes the continuous replenishment of excited state from vibrationally excited (non-radiating) ground state. Inclusion of this type of interaction modifies the interpretation of the observed lifetimes and quenching parameters discussed in the preceding Sections. The quantities derived from the equilibrium model may then be written in terms of the observed values as follows:

$$\tau_R(eq) = \tau_R/(K+1);\ a_V(eq) = a_V/(K+1);\ S(eq) = S(K+1). \qquad (14)$$

Using a value of K = 200 which would ascribe the entire lifetime anomaly to this effect, and using the values of a_V and S obtained from the steady excitation experiments, $\tau_R(eq) = 0.28$ μsec, $a_V(eq) = 3.5$ Torr^{-1}, and $a_E(eq) \leq 7$ Torr^{-1}. For this value of τ_R, $V = 3.9 \times 10^{-10}$ and $E \leq 7.8 \times 10^{-10}$ cm^3/molecule-sec; only an upper limit has been given for E because of the uncertainty in

S. For this high value of K, the equilibrium model results in high quenching rate constants for both vibrational and electronic quenching. However, K should be a measure of the relative degeneracy at equal energies in the excited and ground states. Estimates of this degeneracy ratio give values between about 5 and 30 over the energy range studied. Thus, the equilibrium model is unlikely to provide the sole mechanism of the lifetime lengthening. It is possible, however, that such an equilibrium exists, but that K is, say, 10 or 20, and that other explanations[8] bridge the remaining gap between the radiative lifetime and the integrated absorption coefficient.

Acknowledgements

The authors wish to thank Dr. E. C. Zipf for extensive advice and collaboration on experiments with modulated excitation, and Mr. M. Weinschenker for designing and building the light modulator.

References

* This research was supported by the Advanced Research Projects Agency, The Department of Defense, and was monitored by U. S. Army Research Office - Durham, Box CM, Duke Station, Durham, North Carolina 27706 under Contract No. DA-31-124-ARO-D-440.

† Present address: Singer-General Precision, Inc., Kearfott Division, Little Falls, New Jersey 07424.

1. A. E. Douglas and K. P. Huber, Canadian J. Phys. 43, 74 (1965).

2. L. Burnelle, A. M. May, and R. A. Gangi, J. Chem. Phys. 49, 561(1968); L. Burnelle and K. P. Dressler, J. Chem. Phys. 51, 2758 (1969).

3. W. H. Fink, J. Chem. Phys. 49, 5054 (1968).

4. D. Neuberger and A. B. F. Duncan, J. Chem. Phys. 22, 1693 (1954).

5. T. C. Hall and F. E. Blacet, J. Chem. Phys. 20, 1745 (1952).

6. J. K. Dixon, J. Chem. Phys. 8, 157 (1940).

7. H. P. Broida, H. I. Schiff, and T. M. Sugden, Trans. Faraday Soc. 57, 259 (1961).

8. A. E. Douglas, J. Chem. Phys. 45, 1007 (1966).

9. D. B. Hartley and B. A. Thrush, Discussions Faraday Soc. 37, 220 (1964).

10. G. H. Myers, D. M. Silver, and F. Kaufman, J. Chem. Phys. 44, 718 (1966).

11. K.Sakurai and H. P. Broida, J. Chem. Phys. 50, 2404 (1969).

12. W. P. Baxter, J. Am. Chem. Soc. 52, 3920 (1930).

13. L. F. Keyser, F. Kaufman, and E. C. Zipf, Chem, Phys. Letters 2, 523 (1968).

14. S. E. Schwartz and H. S. Johnston, J. Chem. Phys. 51, 1286 (1969).

15. H. Ishii and K. Nakayama, Trans. Eighth Vacuum Symposium 1, 519 (1961).

16. O. Stern and M. Volmer, Physik. Z. 20, 183 (1919).

17. The possibility that diffusion of excited NO_2 is responsible for the non-linearity at low pressure is unlikely because the curvature changes with $\Delta\nu$. In the low pressure limit where emission occurs from the initially excited level, the effect of diffusion should be independent of the fluorescent wavelength. Moreover, estimated diffusive losses in our sys-

tem are small compared to observed deviation from linearity.

18. A. Fontijn, C. B. Meyer,and H. I. Schiff, J. Chem. Phys. 40, 64 (1964).

19. L. Brewer, C. J. James, R. G. Brewer, F. E. Stafford, R. A. Berg, and G. M. Rosenblatt, Rev. Sci. Instr. 33, 1450 (1962).

20. H. D. Mettee, J. Chem. Phys. 49, 1784 (1968).

21. S. J. Strickler and D. B. Howell, J. Chem. Phys. 49, 1947 (1968).

22. Y. N. Lin and B. S. Rabinovitch, J. Phys. Chem. 72, 1726 (1968); D. C. Tardy, C. W. Larson, and B. S. Rabinovitch, Can. J. Chem. 46, 341 (1968).

23. G. W. Robinson, J. Chem. Phys. 47, 1967 (1967).

24. D. P. Chock, J. Jortner, and S. A. Rice, J. Chem. Phys. 49, 610 (1968).

Table I. Quenching constants, a_{obs}, for steady excitation

	λ_E = 4050Å		λ_E = 4360Å		λ_E = 5460Å		λ_E = 5780Å	
λ_F	$\Delta\nu^*$	a_{obs}, $Torr^{-1}$	$\Delta\nu^*$	a_{obs}, $Torr^{-1}$	$\Delta\nu^*$	a_{obs}, $Torr^{-1}$	$\Delta\nu^*$	a_{obs}, $Torr^{-1}$
4360	1774 cm^{-1}	356						
4700			1656 cm^{-1}	247				
5090	5063	125	3300	160				
5460			4631	129				
5665	7057	107	5294	109				
5990			6252	99	1617 cm^{-1}	362		
6350	8961	73	7198	74	2563	238	1553 cm^{-1}	394
6600			7795	72	3160	207	2150	312
7000	10424	69	8661	64	4026	208	3016	272
7250			9153	63	4518	167	3508	226
7850	11971	69	10208	81	5573	148	4563	195

*$\Delta\nu = \nu_E - \nu_F$

Table II. Values of G(n,S)

n \ S	1.00	0.10	0.01	0.00
1	2.00	1.10	1.01	1.00
2	1.33	.58	.51	.50
3	1.14	.40	.34	.33
4	1.07	.32	.26	.25
5	1.03	.26	.21	.20
6	1.02	.23	.17	.17
7	1.01	.20	.15	.14
8	1.00	.19	.13	.12
9	1.00	.17	.12	.11
10	1.00	.16	.11	.10
12	1.00	.15	.089	.083
14	1.00	.14	.077	.071
16	1.00	.13	.068	.062
18	1.00	.12	.061	.056
20	1.00	.12	.055	.050

Table III. Radiative lifetime and quenching constants of NO_2

λ_E, Å	λ_F, Å	ω, kHz	τ_R, μsec	a_{obs}, $Torr^{-1}$
4360	4700	8	55 ± 2	262 ± 15
4360	4700	8	53 ± 7	262 ± 40
4360	4700	20	54 ± 9	316 ± 65
4360	5990	20	53 ± 3	a
4360	6350	20	54 ± 12	a
5375	5990	8	59 ± 3	224 ± 11
5460	5990	8	58 ± 3	342 ± 25
5780	6350	8	55 ± 3	324 ± 25
5600	CS 2-58[b]	8	54 ± 4	a
6000	CS 2-64[b]	8	53 ± 6	a

[a] $1/\tau$ vs. P plots curved.

[b] Corning sharp cut filters.

Figure Captions

Fig. 1. Diagram of apparatus.

Fig. 2. Diagram of detection system used for lifetime measurements.

Fig. 3. Stern-Volmer plot of representative NO_2 fluorescence results. Excitation wavelength is 4360Å. Theoretical curves calculated for S = 0.01 and $\Delta\nu_{vib}$ = 1000 cm^{-1}.

Fig. 4. Comparison of calculated and experimental relative quenching constants as functions of $\Delta\nu = \nu_E - \nu_F$. Calculated curves obtained using Eq. (5) and Table II; reference value is at $\Delta\nu$ = 1600 cm^{-1}. Excitation wavelength for the experimental points: ● = 4050Å, ○ = 4360Å, △ = 5460Å, and ✕ = 5780Å. Numbers next to curves indicate $\Delta\nu_{vib}$.

Fig. 5. Fluorescent signal waveform; exciting wavelength = 4360Å, fluorescent wavelength = 4700Å at 8.2 mTorr NO_2. Counting time, 8 minutes.

Fig. 6. Reciprocal lifetime vs. pressure of NO_2, exciting wavelength = 4360Å, fluorescent wavelength = 4700Å, 8 kHertz modulation frequency. The line through the points is the least square fit with radiative lifetime = 55 μsec and quenching constant = 262 $Torr^{-1}$.

Fig. 7. Observed lifetime vs. modulation frequency; lifetime calculated using Eq. (13) with τ_1 = 55 μsec and τ_2 = 0.25 μsec. Numbers give fraction of total intensity due to 55 μsec state.

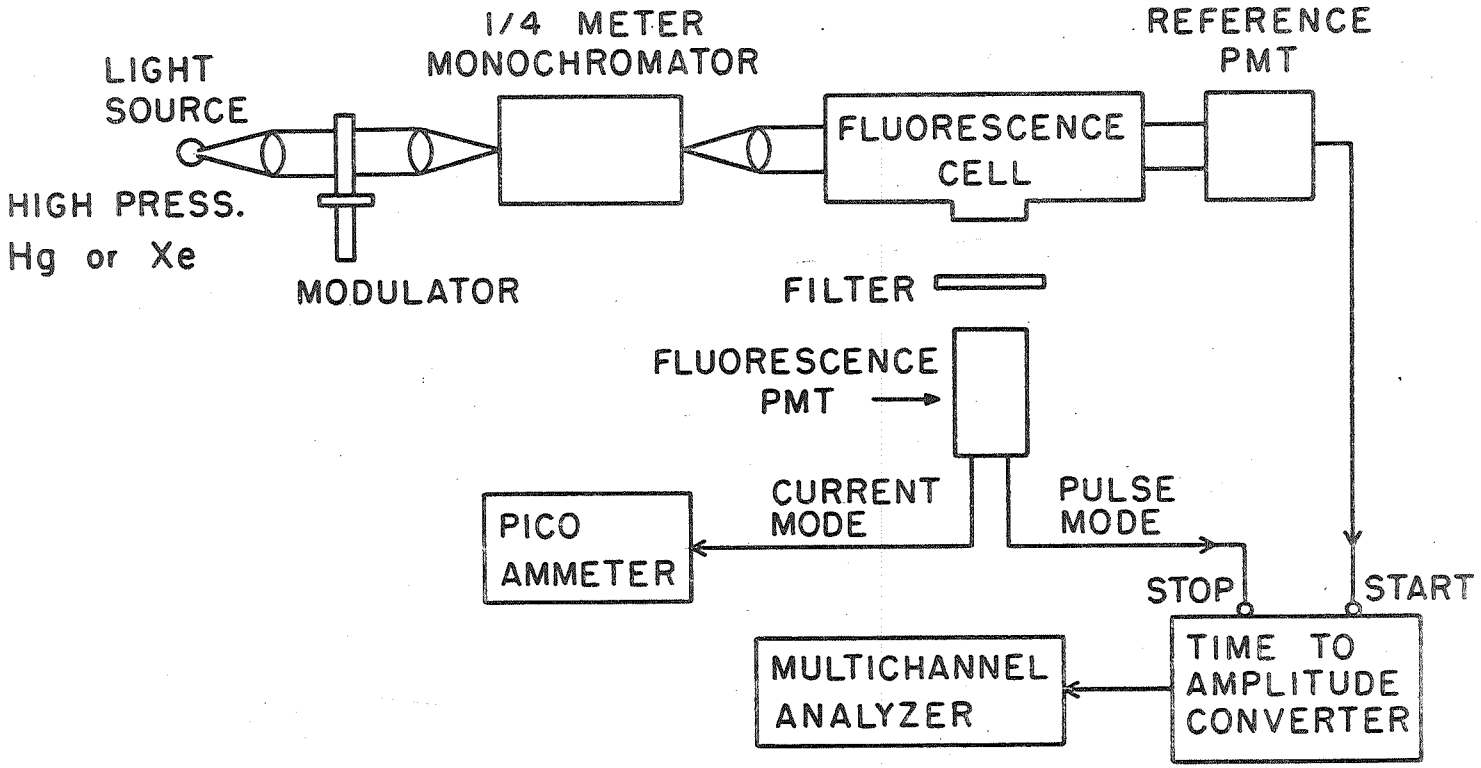
LIGHT SOURCE
HIGH PRESS. Hg or Xe
1/4 METER MONOCHROMATOR
MODULATOR
FLUORESCENCE CELL
REFERENCE PMT
FILTER
FLUORESCENCE PMT
CURRENT MODE
PULSE MODE
PICO AMMETER
STOP
START
TIME TO AMPLITUDE CONVERTER
MULTICHANNEL ANALYZER

Figure 1.

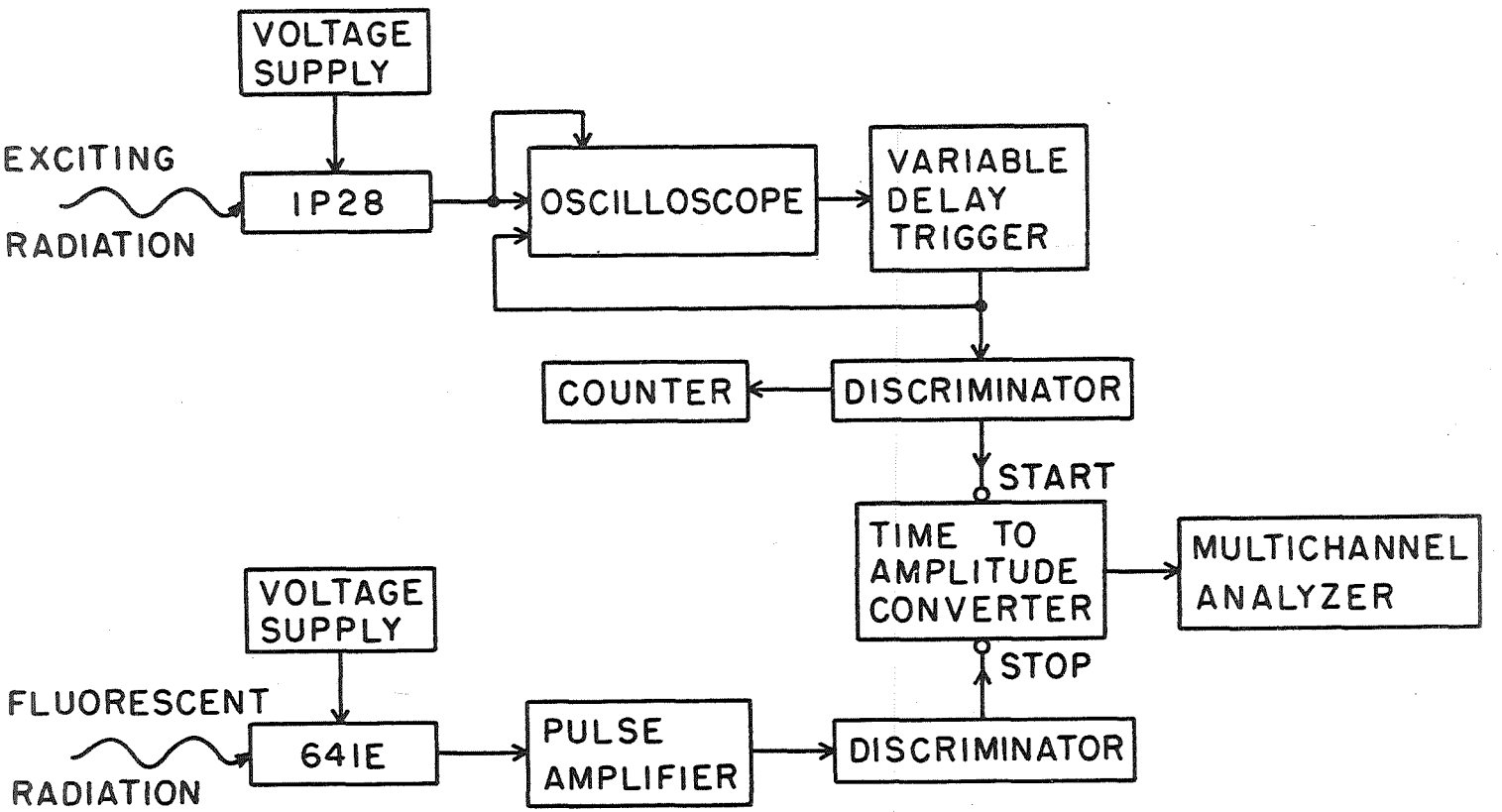
VOLTAGE SUPPLY
EXCITING
RADIATION
IP28
OSCILLOSCOPE
VARIABLE DELAY TRIGGER
COUNTER
DISCRIMINATOR
START
TIME TO AMPLITUDE CONVERTER
MULTICHANNEL ANALYZER
VOLTAGE SUPPLY
FLUORESCENT
RADIATION
641E
PULSE AMPLIFIER
DISCRIMINATOR
STOP

Figure 2.

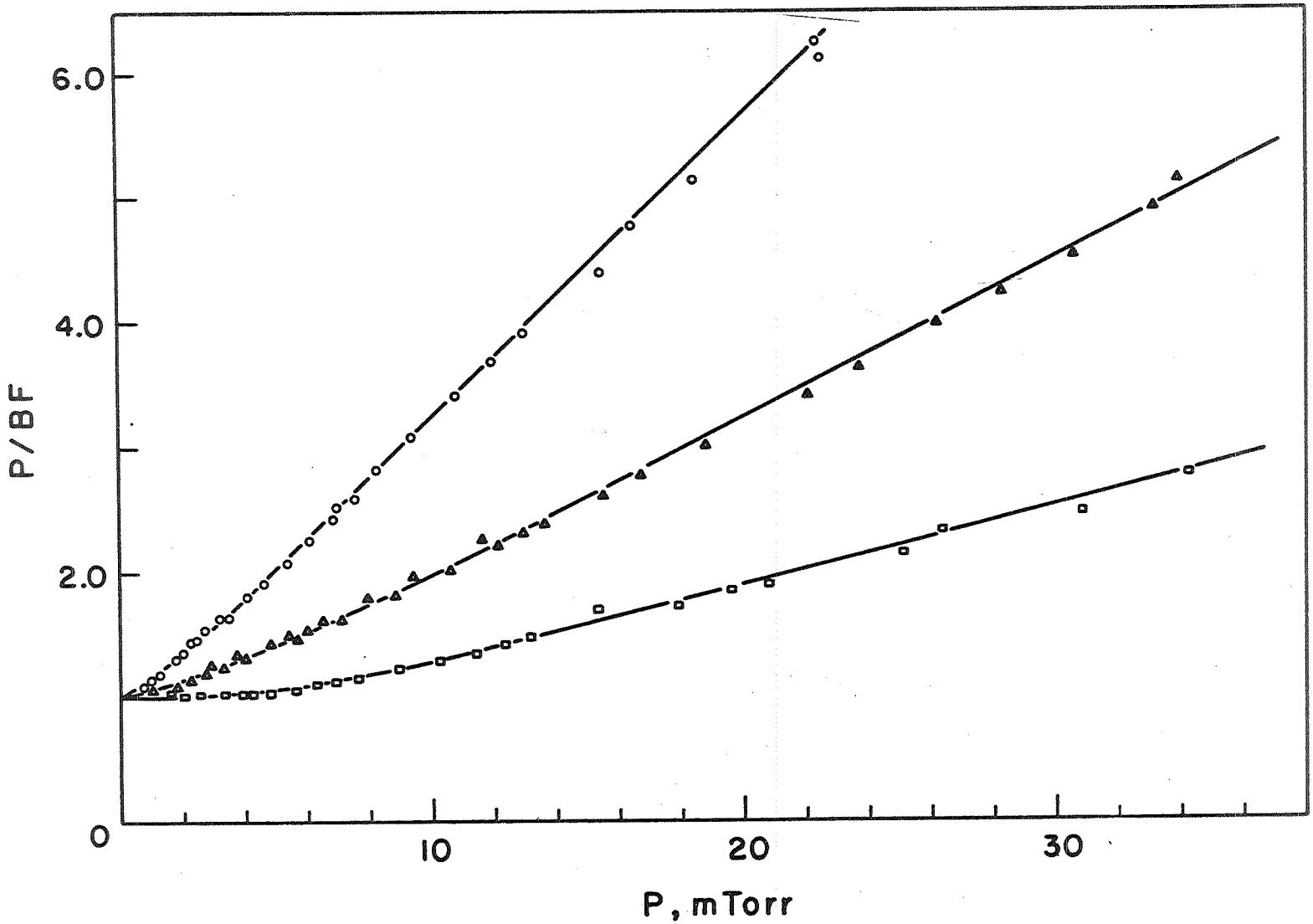

Figure 3.

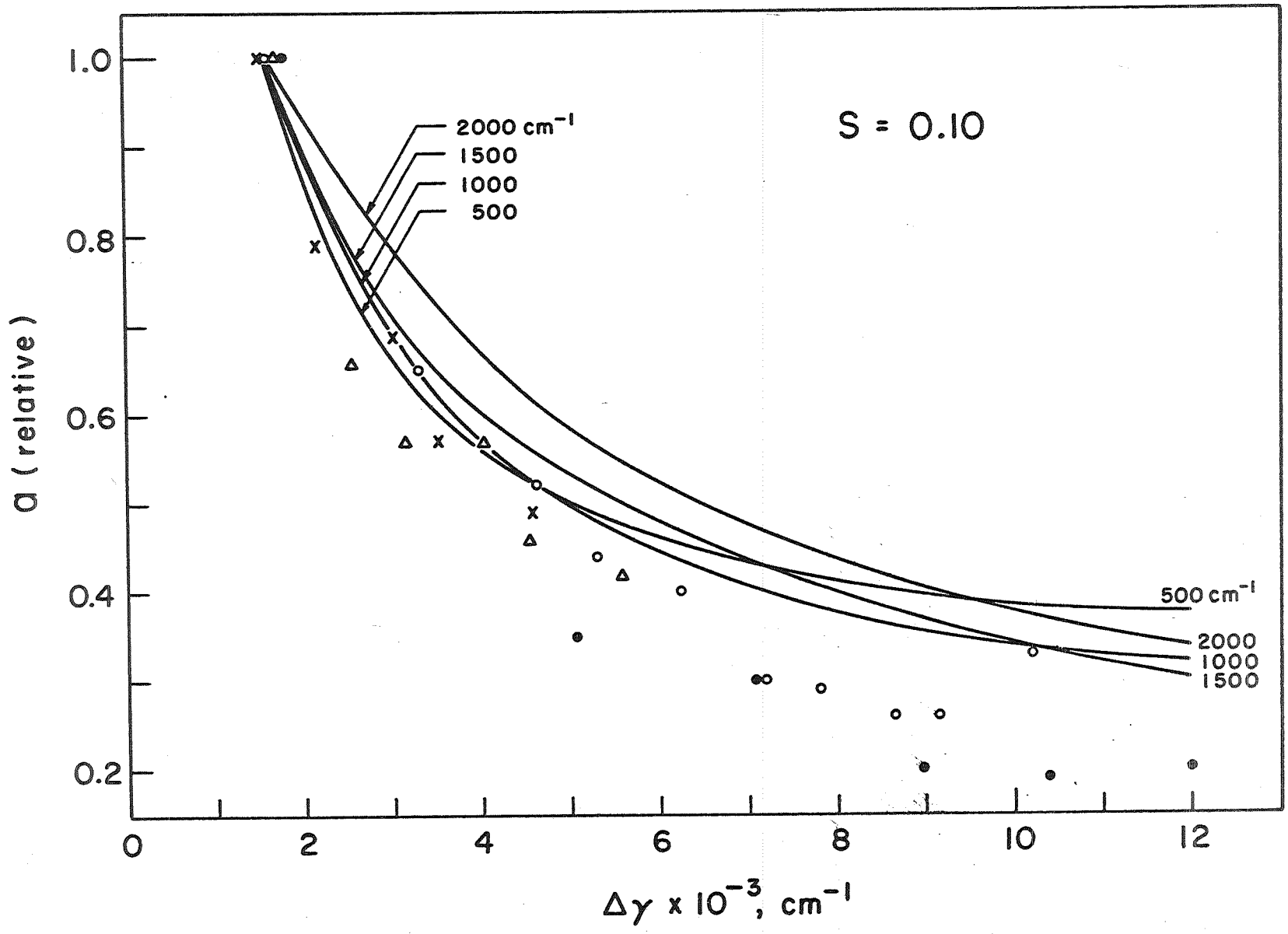
S = 0.10
2000 cm⁻¹
1500
1000
500
500 cm⁻¹
2000
1000
1500
a (relative)
1.0
0.8
0.6
0.4
0.2
0
2
4
6
8
10
12
Δγ x 10⁻³, cm⁻¹

Figure 4a.

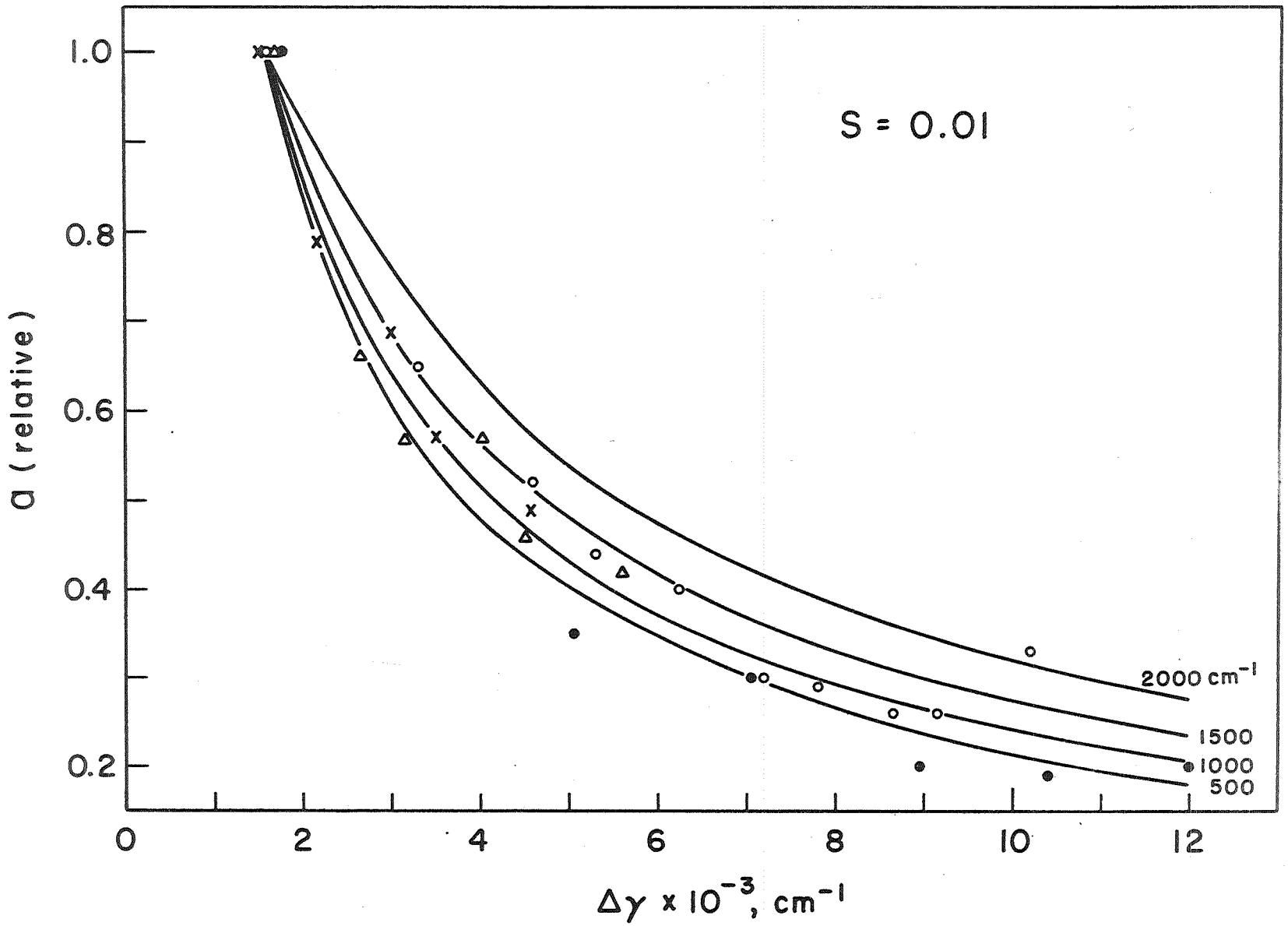
S = 0.01
Q (relative)
1.0
0.8
0.6
0.4
0.2
0
2
4
6
8
10
12
Δγ x 10⁻³, cm⁻¹
2000 cm⁻¹
1500
1000
500

Figure 4b.

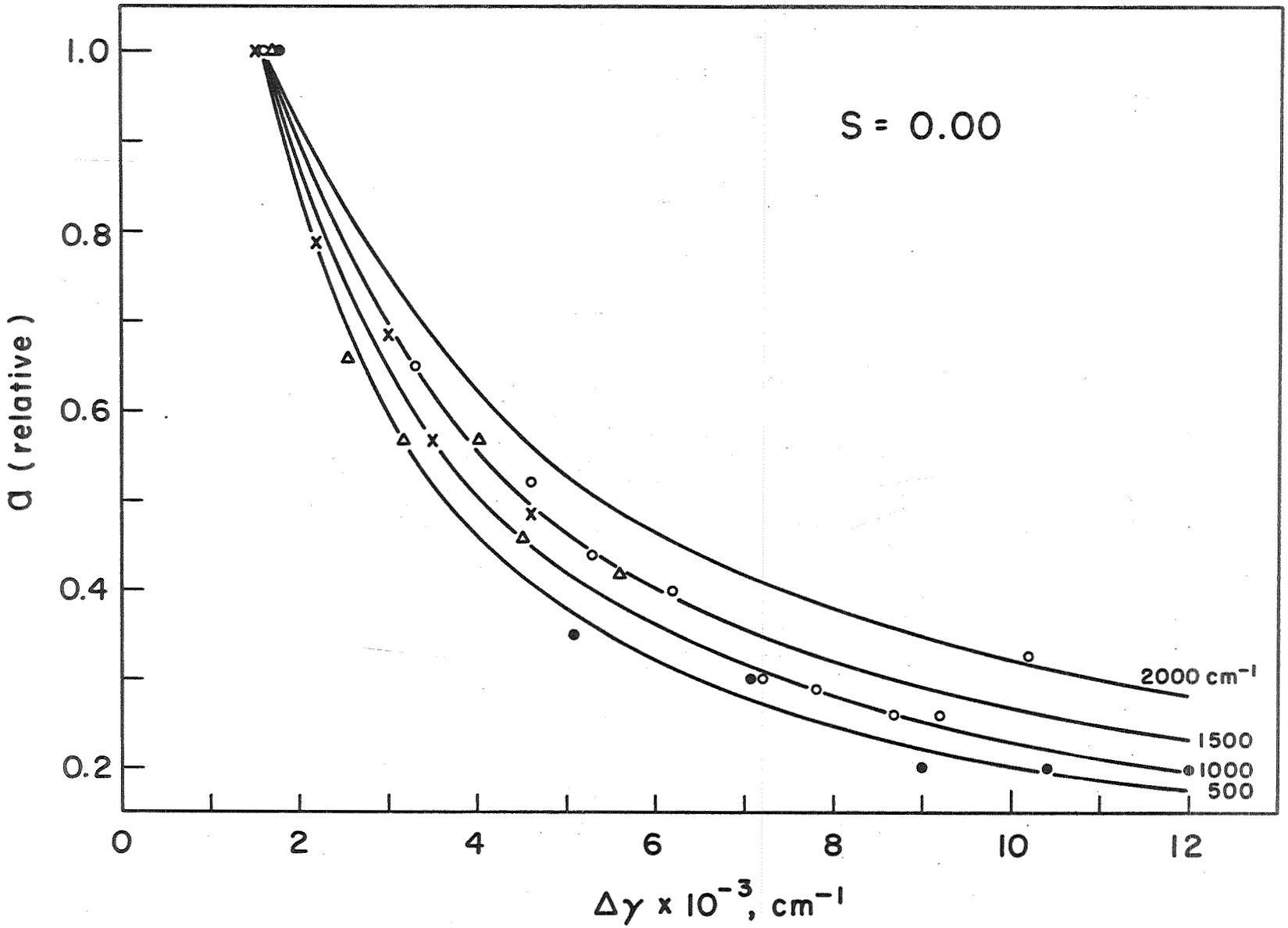
S = 0.00
Q (relative)
1.0
0.8
0.6
0.4
0.2
0
2
4
6
8
10
12
Δγ x 10⁻³, cm⁻¹
2000 cm⁻¹
1500
1000
500

Figure 4c.

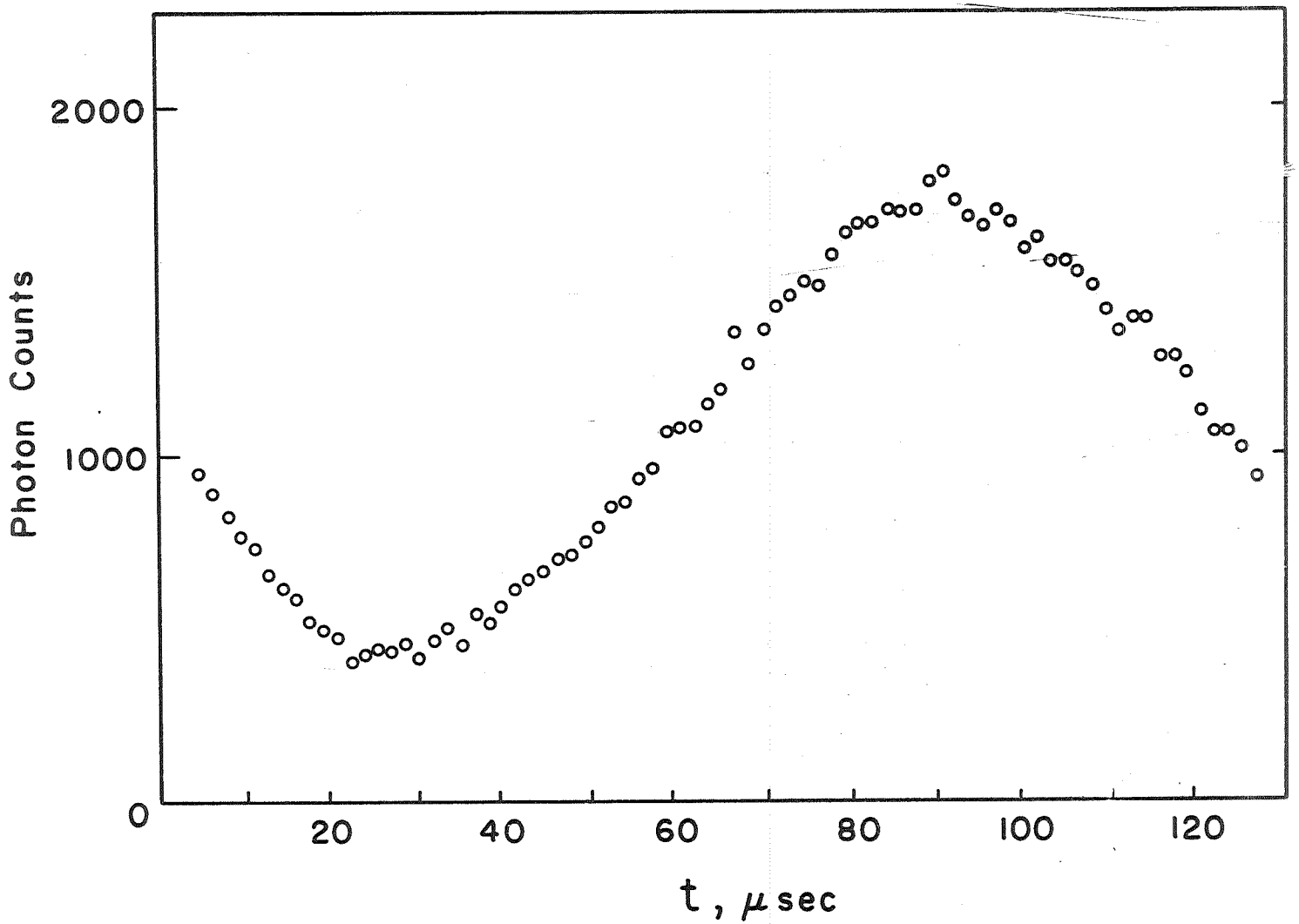

Figure 5.

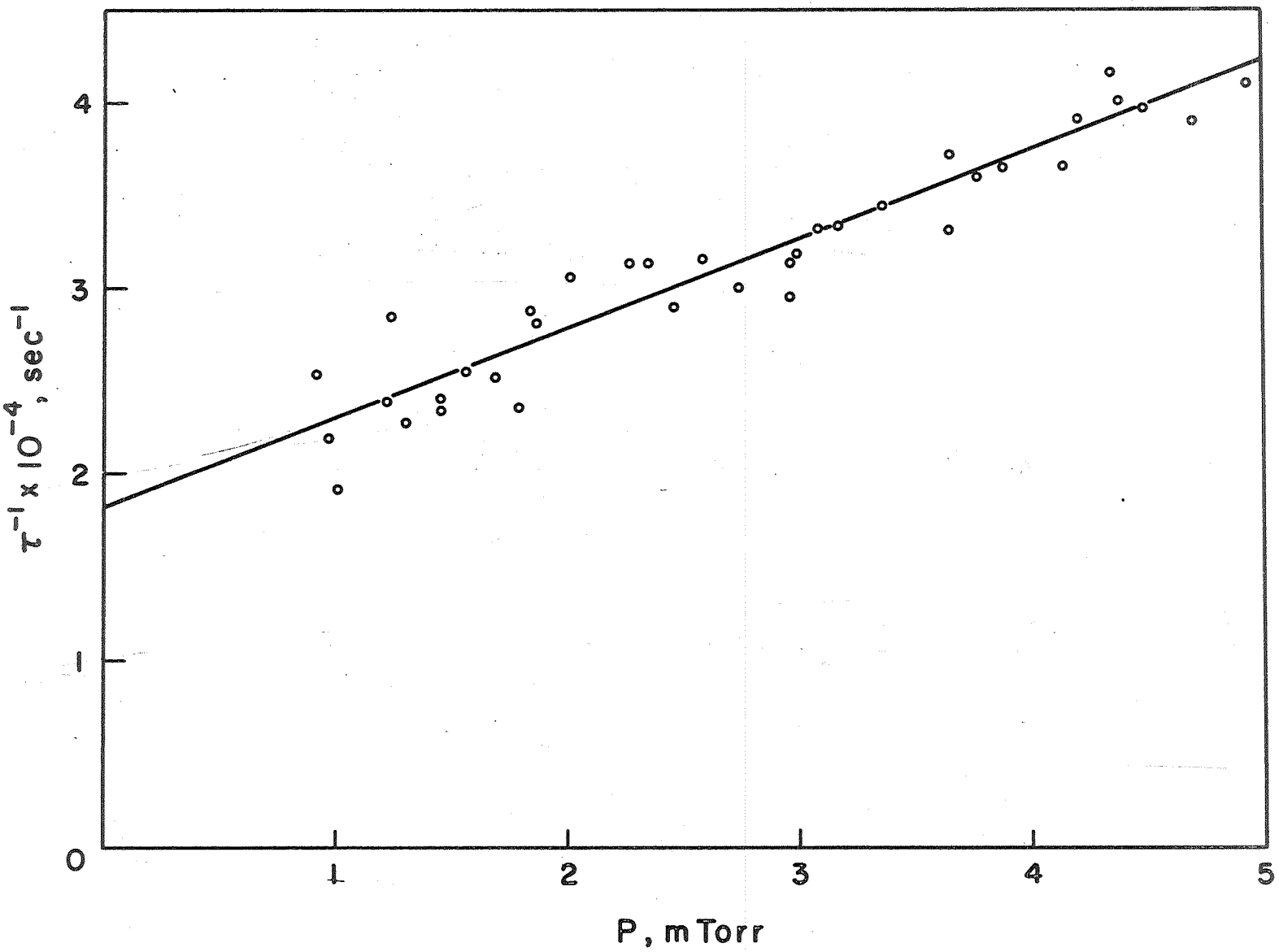

Figure 6.

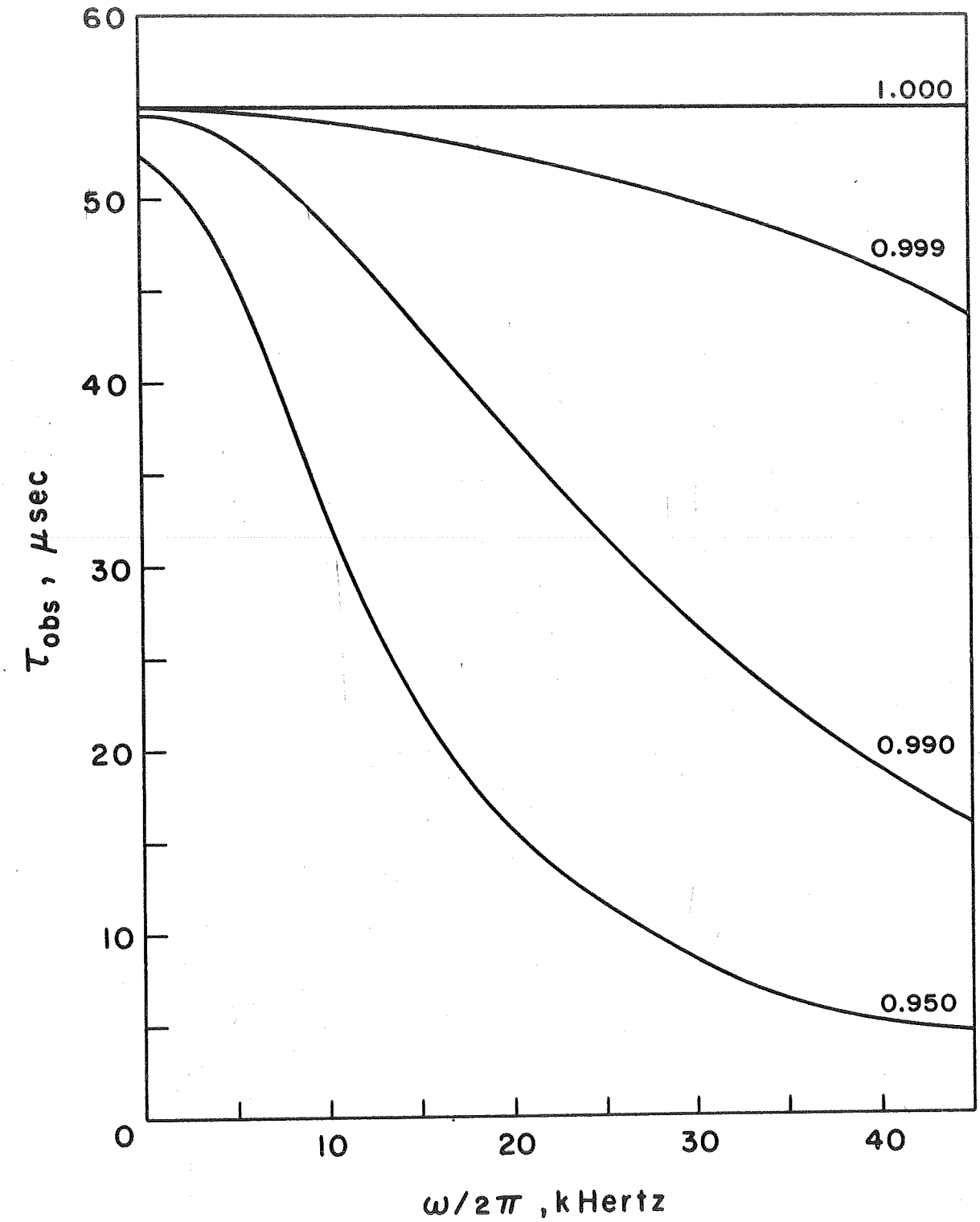
60
50
40
30
20
10
0
1.000
0.999
0.990
0.950
10
20
30
40
τ_{obs} , μsec
$\omega/2\pi$, k Hertz

Figure 7.